

# Human Coronary Artery Lesions: 900 MHz Magnetic Resonance Micro Imaging, NMR Spectroscopy, Histopathology and Oxidative Stress Markers



\*Rakesh Sharma<sup>1,2</sup>

<sup>1</sup>Department of Chemical-Biomedical Engineering, FAMU-FSU College of Engineering, Tallahassee, FL 32304

<sup>2</sup>Hindurao Hospital, Delhi, India

**Submission:** December 27, 2016; **Published:** January 20, 2017

\*Corresponding author: Rakesh Sharma, National High Field Magnetic Resonance Lab, Tallahassee 32304, Florida, Email: rksz2009@gmail.com

## Abstract

**Aim:** 900 MHz Magnetic resonance imaging (MRI) techniques measured the dimensions of atheroma and stenosis in excised human coronary plaque disruption and lipid disorder due to oxidative stress.

**Hypothesis:** Coronary atheroma is a lipid disorder and MRI visible.

**Materials and Methods:** Contiguous cross-sectional T2-weighted fast spin echo MRI images were point-by-point compared with coronary histopathology for quantitation of coronary wall and plaque features. Coronary atheroma tissues were used for NMR spectroscopy and oxidative stress content analysis.

**Results:** 900 MHz MRI images showed distinct measurable wall thickness and vessel radii. The quantitative comparison of lumen areas and wall thickness in endarterectomy specimens using MRI images and histology images showed mean difference 5.0 % for lumen area and 4.5 % for wall thickness. MRI data correlated with the histopathology for aortic wall thickness ( $R^2=0.92$ ,  $P < 0.0001$ ), plaque size ( $R^2=0.99$ ,  $P < 0.0001$ ) and vessel radii ( $R^2=0.79$ ,  $P < 0.0001$ ). MRI images and histological sections showed intraluminal thrombus and plaque disruption. High-resolution NMR peaks suggested the lipid-rich nature of coronary plaque due to presence of triglycerides, phospholipids, sterols and fatty acids. Oxidative stress markers were higher in plaque bearing coronary artery homogenates than the normal coronary artery homogenates. *Ex vivo*, 900 MHz MRI reliably determined the presence, location, and size of the thrombus and % stenosis in coronary artery atherosclerosis and histopathology defined the plaque composition.

**Conclusion:** The study demonstrates the utility of MRI for *in vivo* measurement of % stenosis and distinguishes different components of coronary thrombus *ex vivo* suggesting the coronary artery plaque as a result of lipid disorder and oxidative stress.

**Keywords:** Coronary artery disease; atherosclerosis; MRI; thrombosis; plaque; oxidative stress

## Introduction

Atherothrombotic is a systemic disease of the coronary vessel wall that causes coronary artery lesions appearing heterogeneous in morphology and chemical constitution. Disrupting or vulnerable plaques in the coronary arteries exhibit a thin fibrous cap (fibrous cap thickness 65 to 150  $\mu\text{m}$ ) with a large lipid core, as defined by American Heart Association AHA plaque type V-Va [1]. Acute coronary syndromes often result from disruption of a modestly stenotic vulnerable plaque. Coronary artery vulnerable plaques occasionally show high likelihood of thrombotic complications and rapid progression of

lipid content and a thin fibrous cap [2]. Coronary arteries are thin but their measurements speculate important clinical correlates [3]. Quantitation of the high-risk plaque lipid components and degree of stenosis is state-of-art approach but difficult [4].

However, MRI measures lumen volume, wall thickness, thrombus size, total plaque volume and characterize the composition of the plaques. Noninvasive MRI is emerging tool for identification of flow-limiting coronary Stenoses, calcified plaques, imaging of the atherothrombotic lesions, measurement of atherosclerotic burden, and *ex vivo* characterization of the

coronary plaque components. This combined information for degree of stenosis and the plaque composition, may predict cardiovascular risk, atherothrombotic progression and its response to therapy for the assessment of subclinical disease [5]. The segmentation of coronary plaque MRI images serves to generate plaque feature maps as morphological correlates suggesting heterogeneous nature of coronary plaque [6]. Co registration of MRI images with histopathology stereotactic match may provide validity of quantitation. Oxidative stress causes accumulation of oxidants viz. lipid peroxides and hydro peroxides during atherothrombotic due to lipid disorder [4,6].

The present report focused on application of MRI in stenosis and plaque composition. We measured inner / outer wall perimeters and their radii, plaque features using MRI and histology co registration to calculate wall thickness, thrombus area, lumen size and % stenosis in support of MRI and histological data as possible predictors of stress (higher % stenosis, elevated oxidative stress markers with NMR visible lipid peaks) in different branches due to coronary lipid disorder. We report new approaches of measurement of *in vivo* plaque burden at different branches; better stereotactic visualization of coronary lesion components.

## Materials and Methods

### Ex Vivo 900 MHz MRI and High-Resolution NMR Spectroscopy of Coronary Plaque

10 male human (mean age 45 +/- 4 years) with 30 % - 80 % lumen stenosis participated. 14 coronary artery endarterectomy samples were obtained within 4 hours of cardiac surgery. Severe atherosclerosis and cardiac death were exclusion criteria to select the endarterectomy specimens [3,6]. The area of dissection was defined as a position including right coronary aorta, left anterior descending and circumflex coronary arteries about 10 mm away from the anterior descending artery. The specimens were placed in a device surrounded by phased array surface coil and fast spin echo (FSE) images were acquired at GE Horizon 1.5 T clinical MRI system physiological temperature 37°C as described elsewhere [7].

All research protocols complied with human ethical committee of clinical research. Optimized scan parameters were used to achieve T1, T2 and proton density images of contiguous slices as described elsewhere [8]. Segmentation using SNAKE algorithm was used to quantify wall thickness and coronary artery lumen areas [9]. Segmentation method used delineation and recognition of region and boundaries of vessels in a given scene [10]. To validate the surrogate of truth for comparison, coronary inner and outer wall perimeters were delineated. Adding up plaque or wall areas from 1 mm thick stacked slices provided quantification of plaque constituents [10]. % stenosis and thrombus size was measured as reported elsewhere [10].

High resolution 1-H NMR peaks were obtained in lipid extracts on a Bruker Bios pin 900 MHz magnet housed at

National High Magnetic Field Laboratory, Tallahassee, FL operating at frequency of 900 Hz (21.1 T) after water peak (4.6 ppm) suppression by selective Rf saturation; internal standard  $\text{CHCl}_3$  (7.24 ppm); TR =10 sec; number of FID 64; Fourier Transformed using 16 K points; line broadening 1 Hz; acquisition delay 10  $\mu\text{sec}$ . Peaks were identified on spectra of lipid extracts from coronary plaque tissue based on *a priori* knowledge of their chemical shifts (fatty acid  $\omega\text{-CH}_3$  at ca. 0.86 ppm;  $-(\text{CH}_2)_n$  1.27 ppm;  $=\text{CH-CH}_2$ - methylene at 2.0-2.2 ppm;  $=\text{CH-CH}_2\text{-HC=}$  methylene at 2.75 ppm; vinyl  $-\text{CH=CH-}$  protons at 5.3 ppm; choline head group  $-\text{N}(\text{CH}_3)_3$  at 3.3 ppm of phospholipids; sterol methyl  $18\text{-CH}_3$  - at 0.4 ppm) as previously reported [10,11].

### Coronary Wall and Plaque Measurements

Using *in vivo* MRI images, outer and inner vessel radii measure wall thickness and atheroma size as following and described elsewhere [7]. Wall thickness T can be measured as difference of radii (outer R and inner r) as following equation 1:

$$T = R - r \quad (1)$$

where atheroma size may be calculated based on atheroma length L, atheroma rich area B, and vessel radii as following equation 2:

$$V_{(\text{atheroma})} = L(2R+r).B/6 \quad (2)$$

### Histology of Plaque

Endarterectomy tissue blocks were fixed by immersion in 10 % neutral formalin. Four-micrometer sections comprising all layers of the ventricular wall were stained with Hematoxylin and Eosin with pentachrome [11]. Of the multiple sections of each endarterectomy, one section was randomly analyzed for further morphometric measurements. Optimas 6.5 Image analysis software digitized all arterial segments.

The inner perimeter was defined as the difference of borderlines between lumen and outer vessel wall. Further dividing it by  $2\pi$ , yielded the inner vessel radius. The outer perimeter was defined by the borderline between tunica media and adventitia. The outer vessel radius was obtained by dividing outer perimeter with  $2\pi$ . Wall thickness was computed as the difference between outer vessel radii and inner vessel radii.

### Oxidative Stress Markers

Angiotensin, insulin, Beta-carotene, TBARS, Malonaldehyde (MDA), Vitamin E and C, diene conjugates measured oxidative stress in tissue homogenates of coronary artery segments and control coronary artery segments without plaques as described elsewhere [12].

## Results

### Ex Vivo 900 MHz MRI of Coronary Artery Endarterectomy Specimens

The endarterectomy specimens placed in the close proximity of maximum influence of phased array surface coil magnetic

field generated high signal-to-noise (SNR) ratio. The wall and plaque constituents were distinct on serial MRI images as shown in (Figure 1). Wall thickness and wall radii were calculated by measuring outer wall and lumen perimeters as presented in the (Table 1). Lumen area and thrombus area were delineated and % lumen stenosis was calculated as [area of thrombus / (area of lumen) x 100%]. Outer vessel radius ranged from 1.0-3.5 mm

and wall thickness from 0.1-1.0 mm. Wall thickness, % stenosis and vessel radius comparison is shown in (Table 1 and Figure 2) as regression plots indicating linear relationship. The standard error was 6 % above or below the fitted curve. This relationship was more valid in the large vessels. However, some variation of measurements was also due to anatomical variability of coronary arteries.

**Table 1:** Comparison of histomorphometric measurements and ex vivo 900 MHz MRI visible coronary artery thrombus features of coronary artery serial segments. % aorta wall thickness (mm), atheroma size (mm<sup>2</sup>) and total plaque volume (mm<sup>3</sup>) were measured by superimposed delineation of area on both histology and MRI images in (Figure 1).

| Patient slice <sup>a</sup><br>Patient segment <sup>b</sup> %<br>difference | Coronary artery perimeter   |                             |                                  | Wall<br>thickness<br>(mm) | Wall radius<br>(mm) | % stenosis | Thrombus<br>area (mm <sup>2</sup> ) |
|--|-----------------------------|-----------------------------|----------------------------------|---------------------------|---------------------|------------|-------------------------------------|
|  | Outer<br>(mm <sup>2</sup> ) | Lumen<br>(mm <sup>2</sup> ) | Lumen Area<br>(mm <sup>2</sup> ) |                           |                     |            |                                     |
| A_1  | 17.40                       | 16.33                       | 42.47                            | 0.12                      | 2.78                | 30.47      | 12.94                               |
| A_seg0.5   | 17.34                       | 16.02                       | 40.85                            | 0.11                      | 2.76                | 31.6       | 12.91                               |
| % difference   | 0.35                        | 1.9                         | 3.8                              | 8.3                       | 0.72                | 3.5        | 0.23                                |
| B_4  | 18.10                       | 16.65                       | 44.12                            | 0.23                      | 2.88                | 29.63      | 13.10                               |
| B_seg1.5   | 17.84                       | 15.96                       | 40.53                            | 0.30                      | 2.84                | 32.44      | 13.15                               |
| % difference   | 1.44                        | 4.14                        | 8.14                             | 23.3                      | 1.39                | 8.66       | 0.4                                 |
| C_3  | 19.80                       | 17.09                       | 46.31                            | 0.44                      | 3.15                | 31.3       | 14.50                               |
| C_seg1.5   | 17.60                       | 15.20                       | 36.80                            | 0.38                      | 2.80                | 37.5       | 13.80                               |
| % difference   | 11.1                        | 11.05                       | 20.53                            | 13.6                      | 11.1                | 16.0       | 4.82                                |
| D_6  | 20.60                       | 15.08                       | 36.19                            | 0.88                      | 3.28                | 42.14      | 15.25                               |
| D_seg1.0   | 20.35                       | 13.82                       | 30.41                            | 1.04                      | 3.24                | 49.49      | 15.05                               |
| % difference   | 1.21                        | 8.35                        | 15.9                             | 15.4                      | 1.22                | 14.9       | 1.31                                |
| E_2  | 20.73                       | 15.70                       | 39.27                            | 0.80                      | 3.30                | 46.34      | 18.20                               |
| E_seg2.0   | 20.10                       | 15.08                       | 36.19                            | 0.80                      | 3.20                | 50.15      | 18.15                               |
| % difference   | 3.04                        | 3.95                        | 7.84                             | 0.0                       | 3.0                 | 7.58       | 0.28                                |
| F_4  | 22.11                       | 16.02                       | 40.85                            | 0.97                      | 3.52                | 53.36      | 21.80                               |
| F_seg2.5   | 21.67                       | 15.70                       | 39.27                            | 0.95                      | 3.45                | 55.13      | 21.65                               |
| % difference   | 1.99                        | 1.99                        | 3.86                             | 2.06                      | 1.98                | 3.21       | 0.69                                |
| G_6  | 16.96                       | 11.62                       | 21.50                            | 0.45                      | 2.70                | 42.79      | 9.20                                |
| G_seg2   | 16.02                       | 11.31                       | 20.35                            | 0.75                      | 2.55                | 41.27      | 8.40                                |
| % difference   | 5.54                        | 2.66                        | 5.34                             | 40.0                      | 5.55                | 3.55       | 8.69                                |
| H_8  | 16.65                       | 9.11                        | 13.21                            | 1.20                      | 2.65                | 72.67      | 9.60                                |
| H_seg4   | 15.70                       | 8.80                        | 12.31                            | 1.10                      | 2.50                | 71.08      | 8.75                                |

|              |       |       |       |      |      |       |       |
|--------------|-------|-------|-------|------|------|-------|-------|
| % difference | 6.30  | 3.40  | 6.81  | 8.33 | 1.87 | 2.18  | 8.85  |
| L_4          | 13.19 | 6.79  | 7.33  | 1.02 | 2.10 | 62.07 | 4.55  |
| L_seg2.5     | 12.88 | 6.28  | 6.28  | 1.05 | 2.05 | 70.06 | 4.40  |
| % difference | 2.35  | 7.51  | 14.32 | 2.85 | 2.38 | 11.4  | 1.10  |
| J_10         | 14.45 | 10.05 | 16.08 | 0.70 | 2.30 | 41.98 | 6.75  |
| J_seg3.0     | 14.13 | 10.18 | 16.49 | 0.63 | 2.25 | 39.72 | 6.55  |
| % difference | 2.22  | 1.28  | 2.48  | 10.0 | 2.17 | 5.38  | 2.96  |
| K_12         | 15.70 | 8.73  | 12.14 | 1.11 | 2.50 | 82.37 | 10.00 |
| K_seg3.5     | 15.39 | 8.86  | 12.49 | 1.04 | 2.45 | 78.94 | 9.86  |
| % difference | 1.97  | 1.49  | 2.80  | 6.30 | 2.0  | 4.16  | 1.40  |
| L_14         | 16.65 | 9.39  | 15.09 | 1.10 | 2.65 | 51.68 | 7.80  |
| L_seg4.0     | 16.40 | 9.36  | 13.95 | 1.12 | 1.49 | 46.95 | 6.55  |
| % difference | 1.50  | 0.30  | 7.55  | 1.78 | 43.8 | 9.15  | 16.0  |
| M_3          | 12.25 | 9.74  | 15.09 | 0.40 | 1.95 | 34.46 | 5.20  |
| M_seg1.5     | 12.06 | 9.43  | 14.13 | 0.42 | 1.50 | 36.09 | 5.10  |
| % difference | 1.55  | 3.18  | 6.36  | 4.76 | 23.0 | 4.51  | 1.92  |
| N_5          | 11.62 | 10.05 | 16.08 | 0.25 | 1.85 | 19.90 | 3.20  |
| N_seg2.0     | 11.24 | 9.67  | 15.48 | 0.25 | 1.54 | 20.35 | 3.15  |
| % difference | 3.27  | 3.78  | 3.73  | 0.0  | 15.6 | 2.21  | 1.56  |

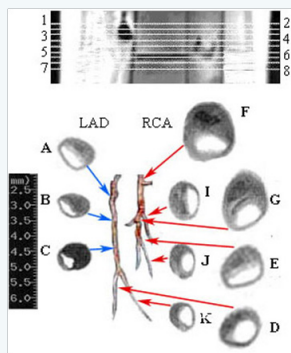


**Figure 1:** A representative ex vivo MRI axial view is shown at different levels (1-8) for coronary endarterectomy coronary artery specimens (panel on top) placed in the close proximity of maximum magnetic field influence of phased array surface coil on its both sides to generate high signal to noise ratio. Notice the different branches of RCA, LAD and LCx coronary arteries showed distinct wall thickening and MRI visible plaque constituents on serial sagittal images in two columns at bottom. RCA branch (D-K) show maximum thickening (right panels at bottom) while LCx and LAD branches (A-C) show lesser thickening (left 3 specimens on left column). For comparison, each coronary image is matched with corresponding histology section shown by side. Notice the histology processing reduces the measurement due to coronary tissue shrinkage.

Coronary artery MRI image mainly defined three morphometric features i.e. lumen area, wall area and plaque area. However, several plaque features viz. lipid core, thrombus, atheroma, calcification, were distinct but not definitive as shown in (Figure 3). Using SNAKE algorithm, wall thickness was measured as shown in (Figure 4).

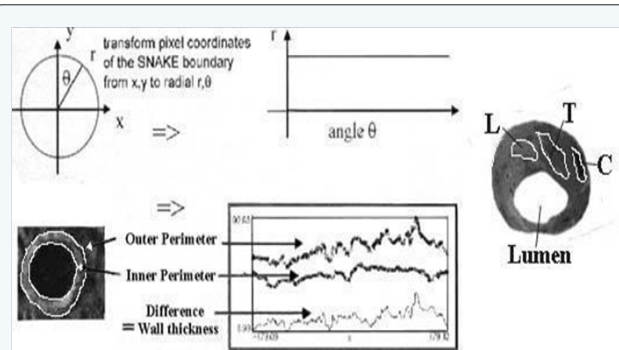


**Figure 4:** The delineation of outer and inner perimeters is shown to measure wall thickness at different points in a coronary artery ex vivo MRI image using SNAKE algorithm (left panel). The delineation of plaque features isointense atheroma (T), darker calcification (C), gray lipid core (L) is shown in a ex vivo MRI image is shown (right panel).

Different levels of MRI image slices showed the in vivo measurements of right coronary artery (RCA), left anterior descending (LAD) and circumflex (LCx) coronary arteries as shown in (Figure 5 and Table 2) indicating RCA at higher risk. Plaque features viz. necrotic core, lipid core, atheroma and wider wall thickness were distinct on MRI images and represented high percent stenosis as shown in (Figure 5). Different wall perimeters, lumen area, wall thickness and thrombus size measurements and their correlation with plaque stability are shown in (Figure 2).

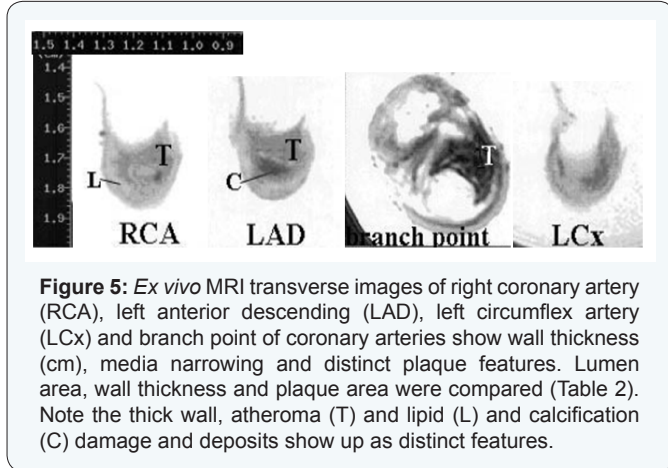
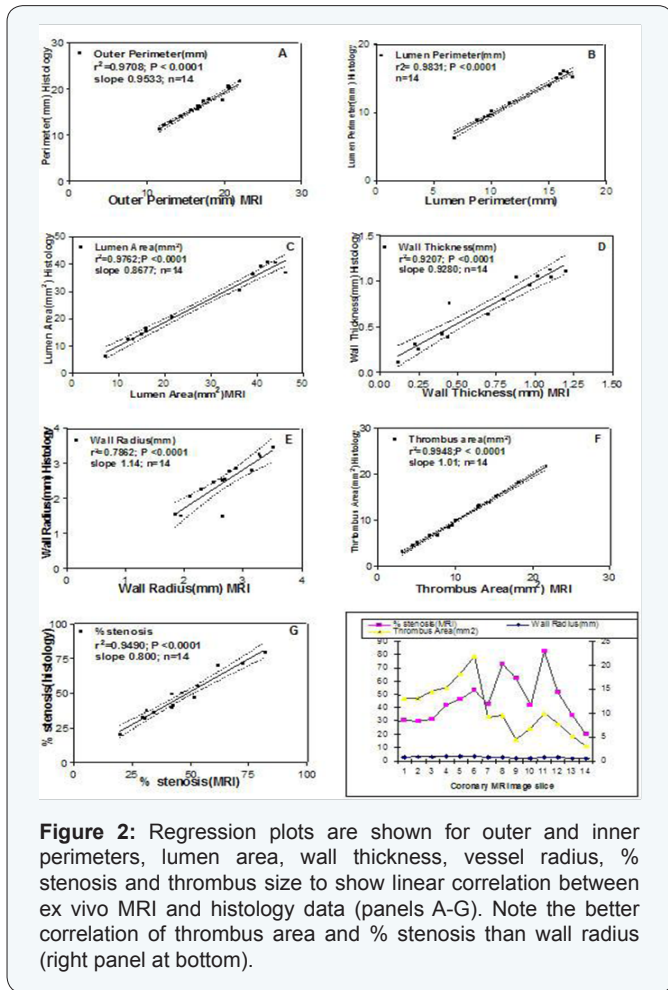
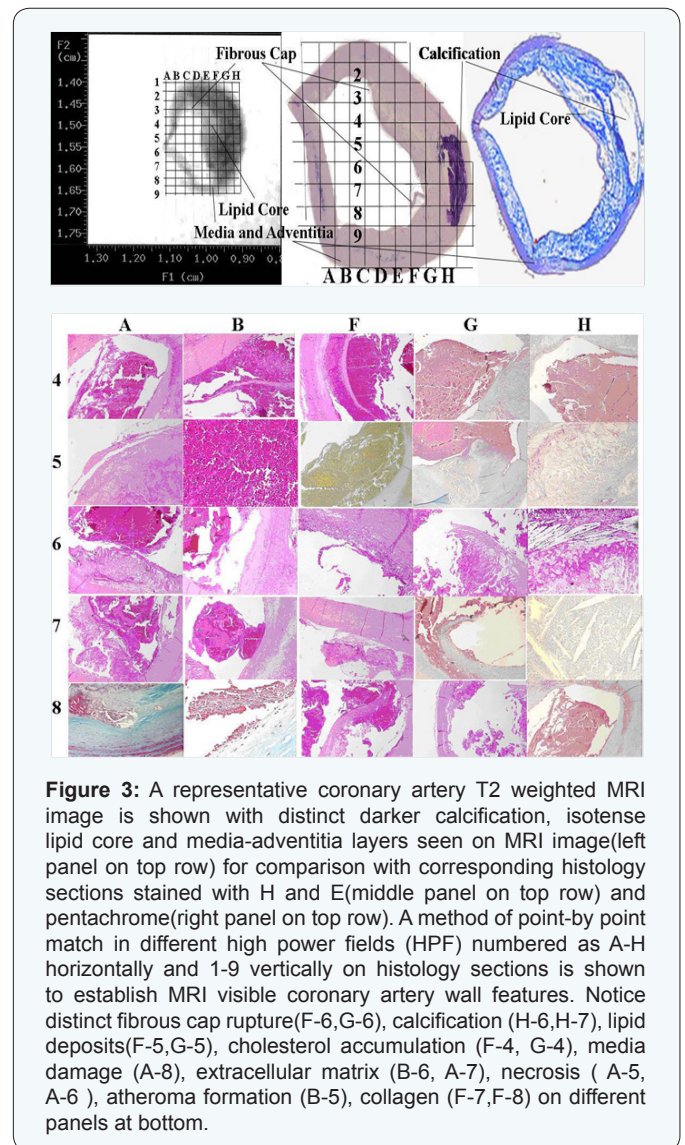


**Table 2:** Lateral difference in RCA, LCx and LAD coronary artery area measurements of a representative endarterectomy specimen # C (Figure 4) for lumen, wall and plaque are shown.

| Plaque Feature                         | RCA   | LCx   | LAD   |
|--|-------|-------|-------|
| Lumen area (mm <sup>2</sup> )          | 40.85 | 16.08 | 15.09 |
| Wall area (mm <sup>2</sup> )           | 36.95 | 5.32  | 8.77  |
| Plaque area (mm <sup>2</sup> )         | 21.80 | 3.2   | 5.2   |
| Lipid core area (mm <sup>2</sup> )     | 6.5   | --    | 2.1   |
| Atheroma area (mm <sup>2</sup> )       | 12.8  | 1.2   | 2.3   |
| Calcification area (mm <sup>2</sup> )  | 4.5   | --    | --    |
| Fibrous tissue area (mm <sup>2</sup> ) | 5.5   | 0.75  | 0.3   |

**Histopathology**



The endarterectomy coronary artery tissues were white with smooth surface. However, permanent fixation in formalin reduced its size due to shrinkage. The histology sections stained

with trichrome-Mason showed microscopic distinct features. The co registration method using 'edge detection' for lumen size, wall thickness, wall radii, and plaque constituents showed % differences by using MRI and histology methods as shown in (Tables 1 & 3) (Figure 6). Histopathology characterized the coronary plaque tissue point-by-point stereotactic match with their MRI signal intensities. On histology sections, lipids, calcification, atheroma, elastin, collagen were main plaque features with fibrous cap, inner wall disruption as shown in different high power fields in (Figure 3).

**Table 3:** High-resolution NMR spectroscopy peak assignments are shown in chloroform extracts of coronary plaque tissues 1-4 (#C,#D,#I and #L). Distinct peak heights at different chemical shift positions suggest protons of specific chemical groups in the lipid-rich plaque constituents as finger prints.

| Lipid NMR peaks                   | Plaque 1 (% stenosis >60%) | Plaque 2 (% stenosis <50%) | Plaque 3 (% stenosis >70%) | Plaque 4 (% stenosis >50%) |
|-----------------------------------|----------------------------|----------------------------|----------------------------|----------------------------|
| $\omega$ -CH <sub>3</sub>         | 12.3                       | 8.2                        | 12.7                       | 10.0                       |
| -(CH <sub>2</sub> ) <sub>n</sub>  | >15                        | 14                         | >15                        | 15                         |
| =CH-CH <sub>2</sub> -             | 4.1                        | 1.3                        | 2.9                        | 2.0                        |
| =CH-CH <sub>2</sub> -HC=          | 3.5                        | -                          | -                          | 0.7                        |
| =CH-CH <sub>2</sub> -HC=          | 2.5                        | 1.5                        | 3.0                        | 1.8                        |
| -N(CH <sub>3</sub> ) <sub>3</sub> | 1.1                        | 0.5                        | 10.0                       | -                          |
| 18-CH <sub>3</sub> -              | 7.2                        | 4.5                        | 6.4                        | 5.8                        |

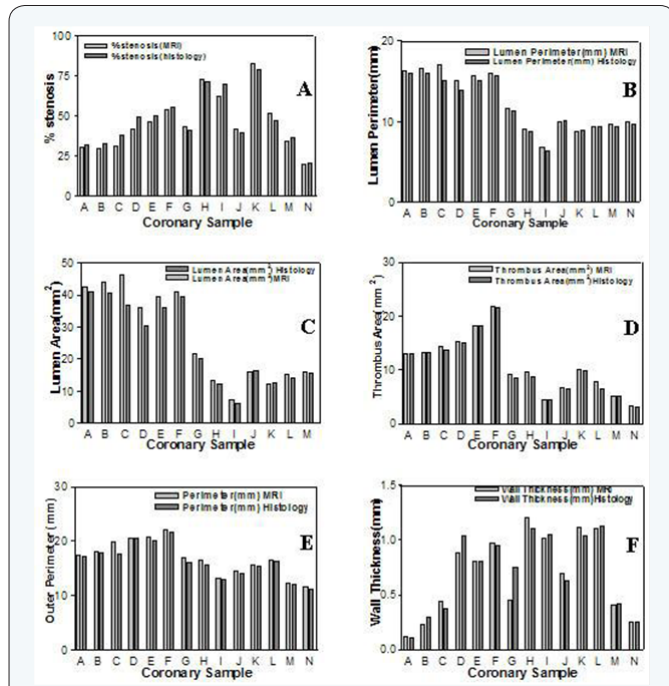


**Figure 6:** Different histogram bars (1-6) represent *ex vivo* MRI data and histology data (A-L) of different coronary artery tissues as shown in Table 1. Comparison is shown in % difference for different measurements.

A. High-Resolution NMR Spectroscopy of Coronary Plaques: Fatty acid moieties of triglycerides, phospholipids, and cholesterol esters were prominent contributors to the observed proton resonances peaks identified on spectra of lipid extracts from coronary plaque tissue. The peaks showed chemical shifts (fatty acid  $\omega$ -CH<sub>3</sub> at 0.86 ppm; -(CH<sub>2</sub>)<sub>n</sub> 1.27 ppm; =CH-CH<sub>2</sub>- methylene at 2.0-2.2 ppm; =CH-CH<sub>2</sub>-HC= methylene at 2.75 ppm; vinyl =CH-CH<sub>2</sub>-HC= protons at 5.3 ppm; choline head group -N(CH<sub>3</sub>)<sub>3</sub> at 3.3 ppm of phospholipids; sterol methyl 18-CH<sub>3</sub>- at 0.65 ppm based on a priori knowledge of these peak positions as shown in (Figure 7). However, other unidentified peaks at 0.95, 1.5, 2.0, 4.1 and 4.2 were also accountable as shown in (Figure 7).

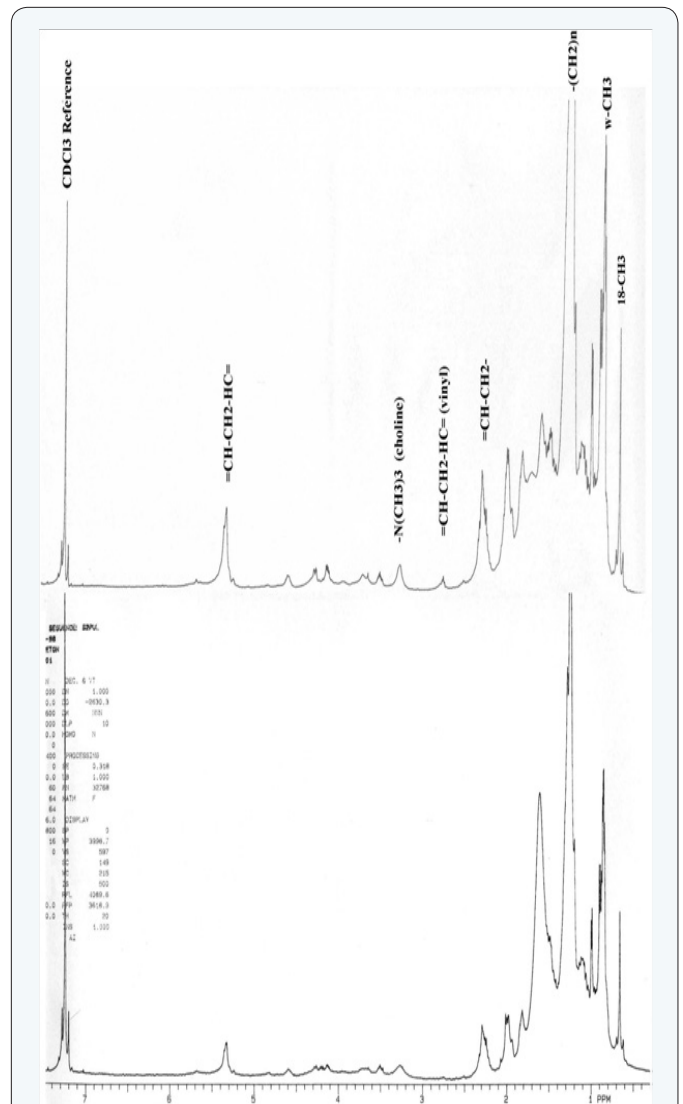


**Figure 7:** High-resolution NMR spectroscopy peak assignments are shown in chloroform extracts of coronary plaque tissues (#G and #L). Distinct peak heights at different chemical shift positions suggest the lipid-rich plaque constituents as finger prints. However, some NMR peaks remained unidentified.

B. Oxidative Stress Markers: Coronary artery normal tissues and atheroma bearing tissue homogenates showed distinct and comparable high values of angiotensin, insulin, beta-carotene, vitamins C and E, TBARS, MDA, diene conjugates contents as shown in (Table 4).

**Table 4:** Oxidative stress marker atheroma constituents are shown in normal and atheroma in coronary tissues. These constituents are represented in international units for comparison.

| Oxidative stress constituent | % difference from Normal Coronary aorta | Coronary atheroma |
|------------------------------|---|-------------------|
| Angiotensin                  | + 25.5                                  | 45.8+/-13.7       |
| Beta-carotene                | - 38.5                                  | 0.6+/-0.09        |
| TBARS                        | + 55                                    | 1.58+/-0.30       |
| Cholesterol                  | + 35                                    | 4.2+/-0.39        |
| Triglycerides                | + 42                                    | 2.84+/-0.33       |
| MDA                          | + 39                                    | 2.45+/-0.55       |
| Diene conjugates             | + 58                                    | 30.8+/-2.97       |
| Insulin                      | + 13.8                                  | 0.18+/-0.11       |
| Vitamin C                    | - 14                                    | 1.05+/-0.14       |
| Vitamin E                    | - 25.5                                  | 2.15+/-0.44       |

However, cholesterol and triglycerides were similar in both homogenates as shown in (Figure 7). Very often, high % stenosis > 60 % and bigger atheroma size were associated with  $-(CH_2)_n$ , 18-CH<sub>3</sub>- sterol peak, choline head group  $-N(CH_3)_3$  NMR peaks and higher oxidative stress markers viz. TBARS, MDA, diene conjugates in cholesterol rich plaques common in RCA tissues. Less vulnerable plaques however showed  $=CH-CH_2-$  methylene,  $=CH-CH_2-HC=$  NMR peaks with comparable oxidative markers common in LAD and LCx tissues. However, it did not rule out the possibility of other plaque lipids.

## Discussion

Coronary atheroma is the consequence of lipid disorder and continuous oxidative stress that leads to plaque disruption. We believe that the size of atheroma and % stenosis serve as morphometric indices measured as wall thickness and lumen area. Further, plaque features such as disruption, fibrous cap, calcium and lipid deposits earlier highlighted the physiochemical processes in coronary wall [1-4,13,14]. In same direction, the present study demonstrated the enhanced power of MRI as tool of MRI-visible coronary vessel morphometric measurements and plaque constituents to evaluate degree of stenosis and thrombosis. It highlighted the use of phased array coil to get combined T1 weighted, T2 weighting and proton-density weighted images in wall visualization and validated the multicontrast MRI signal intensities of different coronary plaque components at various locations.

## Multicontrast MR Plaque Imaging

MR micro imaging is emerging as the potential noninvasive ex vivo MR imaging modality. MR techniques differentiate plaque components on the basis of biophysical and biochemical coronary tissue properties such as chemical composition, chemical concentration, water content, physical state, molecular motion, or diffusion. In present study, ex vivo MR coronary artery imaging utilized a multi-contrast approach with high-resolution black blood spin echo- and fast spin echo (FSE)-based MR sequences [15]. The signal from the blood flow is rendered black through preparatory pulses (e.g. radiofrequency spatial saturation or inversion recovery pulses) to improve the image of the adjacent vessel wall. However, bright blood imaging by 3D Fast time-of-flight pulse sequence was also employed in assessing fibrous cap thickness and morphological integrity of the coronary artery. This sequence enhanced the signal from flowing blood and a mixture of T2\* and proton density contrast weighting highlighting the fibrous cap. Atherosclerotic plaque composition by MRI is generally based on the signal intensities and morphological appearance of the plaque on T1 weighted, proton density-weighted, and T2-weighted images as previously validated [13,14]. Optimized scan parameters and combined weighting generate good contrast for coronary artery features. However, this weighting scheme for imaging may suffer from plaque semi liquid phase and its fatty esters in cholesterol-rich moiety whose saturated/unsaturated lipid ratio determines the severity of disease and plaque stability [12,16]. Therefore, delineation and feature visual identification of coronary vessel constituents may serve the purpose to some extent.

## Ex Vivo 900 MHz MR Micro imaging of Human Coronary Arteries and Aorta Histopathology Correlation

Adventitia and thin layer of innermost media were poorly visible in coronary specimens. These observations corroborate with earlier report on thin fibrous cap, respiratory motion, and poor lipid rich moiety as factors for T2-weighted MRI visibility or Contrast Noise Ratio (CNR) of lumen narrowing [13,14]. In present study, short T2 plaque components were MR visible such as calcification and thrombus. These components were quantified in vivo before surgery procedure and correlated with coronary artery lesion size obtained ex vivo after surgery. The quantification of lesion size, detection of media thickness and fibrous cap 'integrity' evaluations were main focus. In present study, the images were acquired with a resolution of 0.25 x 0.25 x 2.0 to 0.4 x 0.4 x 3.0 mm<sup>3</sup> by use of a coronary phased-array coil to improve signal-to-noise ratio and image resolution. A recent report reviewed the data on coronary aorta composition and atheroma size with the use of T1-weighted, T2-weighted, and proton density-weighted images at a resolution of 0.8 x 0.8 x 5.0 mm<sup>3</sup> using a phased array coil-high-resolution imaging or contrast-enhanced MRA by gadolinium-based contrast agents for plaque neovascularization, necrotic core and fibrous tissue [14].

In present study, SNAKE contour algorithm demarcated the distinct lumen and artery wall boundaries in less time to measure all of the coronary artery size. Coronary artery wall thickness and areas in CAD were greater than normal coronary artery. Different branches of coronary artery showed similar relationship. The correlation of coronary artery wall and plaque measurements by MRI and histology methods offered comparison as % difference <6 % and demonstrated the thrombus area as better plaque stability indicator over wall thickness. It supported other previous report [15].

The plaques features such as lipids, calcification, atheroma, elastin and collagen were main plaque features. Fibrous cap, inner wall disruption were quite distinct on histology sections but on MRI images only different signal intensities suggested presence of different components due to limited MRI resolution. So, we suggest combined information on wall morphology and plaque features offer better sensitivity and specificity with possibility of cardiovascular risk.

### **Sensitivity and Specificity of Coronary MRI (Stenoses: > 50%)**

The present study suggested the % stenosis based on our new technique [7] to measure wall radii and lumen size as possible cardiovascular risk marker (no risk with 30-39 % stenosis; prone to risk with 40-50 % stenosis; mild risk with 50-69 % stenosis; unstable or vulnerable plaque with 70-79% stenosis; high risk with 80 % stenosis or above). However, wall thickness also appeared as better risk correlate. Our results support the previous investigations predicting >50 % stenosis as considerable risk [15,17]. The current state-of-art using several modified MR pulse sequences suggested further improvement in specificity and sensitivity of techniques used.

### **Coronary Plaque Lipids with High Resolution NMR Spectroscopy**

Saturated and mono- or polyunsaturated ( $\omega$ -3 or  $\omega$ -6 esters) of fatty acid rich phospholipids and triglycerides as major coronary lipids have been reported by high resolution NMR as fingerprints [18,16] and partial lack of lipid molecule mobility was attributed for their accumulation around coronary wall. It is a disadvantage in clinical time-dependent assessment of lipids during plaque progression. Presence of high-saturated lipids and free cholesterol contents reduce the plaque stability or cause adverse consequence [5,16].

### **Coronary Oxidative Stress Markers**

Triglycerides, cholesterol, insulin and angiotensin converting Enzyme in the atheroma are believed as indicators of plaque severity and extent of atherosclerosis. Malonaldehyde, TBARS, and diene conjugates serve as indicators of free radical damage in artery. Beta-carotene, vitamin E and C decrease with increased free radical damage and plaque severity indicates coronary artery at high risk of atheroma. The increased atheroma biochemical precursors and NMR lipid peaks in artery homogenates

indicated the coronary artery disease as consequence of lipid accumulation in walls or plaques within arteries. Both NMR and oxidative stress data suggested atherosclerosis as a lipid disorder [16,18,19]. Moreover, it gave a window to understand further the possible role of oxidative stress in atheroma formation. In control coronary tissue homogenates, indirect measures of oxidatively damaged lipids indicated the lesser free radical stress or no stress [5]. Higher concentrations of TBARS indicating high oxidative activity have been observed in coronary artery disease [6]. Higher triglyceride concentrations compared to cholesterol in CAD tissue homogenates may be due to less hydrolysis of triglycerides into fatty acids.

### **Limitation of this Study**

Limitation of this study was that ex vivo investigations of endarterectomy coronary artery material changed the morphometric data during fixation and tissue processing such as shrinkage artifacts during dehydration. Other factors were limited lipid discrimination on MRI images due to vessel small size, hyper contracture of vessels and wall tension considerations while evaluating plaque vulnerability. Some notable improved blood suppression methods are reported for accurate coronary plaque imaging by dual-inversion 3D FSE imaging sequence with real-time navigator technology for high-resolution, free-breathing black-blood CMRA [20], delineation of coronary artery by echo planar imaging [21], MRA and True FISP imaging [22,23].

### **Conclusion**

Multicontrast MR imaging may measure dimension of coronary stenoses in different branches. MRI may visualize the coronary plaque disruption and atherosclerotic lesion components, measuring atherosclerotic burden comparable with histological features. Relationship of outer vessel radius and wall thickness, plaque atheroma size and % stenosis might serve as clinical correlates of cardiovascular risk, its response to therapy and assessment of subclinical disease. These results indicate possibility of coronary stenosis and thrombosis due to oxidative stress and lipid disorder.

### **Acknowledgement**

Author acknowledges the atherosclerosis training and methods adopted for MRI images in (Figures 1,4, and 5) as pilot experiments.

### **References**

1. Naghavi M, Libby P, Falk E, Casscells SW, Litovsky S, et al. (2003) From vulnerable plaque to vulnerable patient: a call for new definitions and risk assessment strategies: Parts I and II. *Circulation* 108(14): 1764-1778.
2. Erbel R, Ge J, Gorge G, Baumgart D, Haude M, et al. (1999) Intravascular ultrasound classification of atherosclerotic lesions according to American Heart Association recommendation. *Coron Artery Dis* 10(7): 489-499.
3. Podesser BK, Neumann F, Neumann M, Schreiner W, Wollenek G, et al. (1998) Outer radius-wall thickness ratio, a postmortem quantitative histology in human coronary arteries. *Acta Anat (Basel)* 163(2): 63-68.



4. Witztum JL (1994) The oxidative hypothesis of atherosclerosis. *Lancet* 344: 793-796.
5. Singh RB, Dubnov G, Niaz MA, Ghosh S, Singh R, et al. (2002) Effect of an Indo-Mediterranean diet on progression of coronary artery disease in high risk patients(Indo-Mediterranean Diet Heart Study): a randomised single-blind trial. *Lancet* 360(9344):1455-1461.
6. Niato C, Kawamura M, Yamamoto Y (1993) Lipid peroxides as the initiating factor of atherosclerosis. *Ann NY Ac ad Sci* 676: 27-45.
7. Sharma R (2002) A device for MR imaging of atherosclerosis plaque in carotid endarterectomy specimens ex vivo. *Magn Reson Med Sci* 1(2): 129-136.
8. Morrisett J, Vick W, Sharma R, Lawrie G, Reardon M, et al. (2003) Discrimination of components in atherosclerotic plaques from human carotid endarterectomy specimens by MRI in vivo. *Magn Reson Imaging* 21(5): 468-474.
9. Sharma R, Singh RB, Gupta RK (2003) A Segmentation method for Carotid Artery Atherosclerosis Plaque for MRI contrast and Oxidative Stress markers in plaque. *Proceedings 16th IEEE Symposium on Computer-Based Medical Systems* June 26 - 27, 2003 Mt Sinai Hospital, New York, New York Ed Krol M 16: 323-328.
10. Cline HE, Thedens DR, Irrarrazaval P, Meyer CH, Hu BS, et al. (1998) 3D MR coronary artery segmentation. *Magn Reson Med* 40(5): 697-702.
11. Pearlman JD, Zajicek J, Merickel MB, Carman CS, Ayers CR, et al. (1988) High-resolution 1H NMR spectral signature from human atheroma. *Magn Reson Med* 7(3): 262-279.
12. Singh RB, Shinde SN, Chopra RK, Niaz MA, Thakur AS, et al. (2000) Effect of coenzyme Q10 on experimental atherosclerosis and chemical composition and quality of atheroma in rabbits. *Atherosclerosis* 148(2): 275-282.
13. Yuan C, Hatsukami TS, O'Brien KD (2001) High-Resolution magnetic resonance imaging of normal and atherosclerotic human coronary arteries ex vivo: discrimination of plaque tissue components. *J Investig Med* 49(6): 491-499.
14. Fayad ZA, Choudhury RP, Fuster V (2003) Magnetic resonance imaging of coronary atherosclerosis-Review. *Current Atheroscler Report* 5(5): 411-417.
15. Worthley SG, Helft G, Fayad ZA, Fuster V, Rodriguez OJ, et al. (2001) Cardiac gated breath-hold black blood MRI of the coronary artery wall: an in vivo and ex vivo comparison. *Int J Cardiovasc Imaging* 17(3): 195-201.
16. Pella D, Dubnov G, Singh RB, Sharma R, Berry EM, et al. (2003) Effects of an Indo-Mediterranean diet on the omega-6/omega-3 ratio in patients at high risk of coronary artery disease: the Indian paradox. *World Rev Nutr Diet* 92:74-80.
17. Fayad ZA, Fuster V, Nikolaou K, Becker C (2002) Computed tomography and magnetic resonance imaging for noninvasive coronary angiography and plaque imaging: current and potential future concepts. *Circulation* 106(15): 2026-2034.
18. Zajicek J, Pearlman JD, Merickel MB, Ayers CR, Brookeman JR, et al. (1987) High-resolution proton NMR spectra of human arterial plaque. *Biochem Biophys Res Commun* 149(2): 437-442.
19. Duerinckx AJ (2001) Imaging of coronary artery disease-Review. *MR. J Thorac Imaging* 16(1): 25-34.
20. Botnar RM, Stuber M, Kissinger KV, Kim WY, Spuentrup E, et al. (2000) Noninvasive coronary vessel wall and plaque imaging with magnetic resonance imaging. *Circulation* 102(21): 2582-2587.
21. Deshpande VS, Li D (2003) Contrast-enhanced coronary artery imaging using 3D true FISP. *Magn Reson Med* 50(3): 570-577.
22. Stehning C, Boerner P, Nehrke K (2007) Advances in coronary MRA from vessel wall to whole heart imaging. *Magn Reson Med Sci* 6(3): 157-170.
23. McCarthy RM, Deshpande VS, Beohar N, Meyers SN, Shea SM, et al. (2007) Three-dimensional breathhold magnetization-prepared True FISP: a pilot study for magnetic resonance imaging of the coronary artery disease. *Invest Radiol* 42(10): 665-670.



This work is licensed under Creative Commons Attribution 4.0 License  
DOI: [10.19080/JOCCT.2017.03.555602](https://doi.org/10.19080/JOCCT.2017.03.555602)

### Your next submission with Juniper Publishers will reach you the below assets

- Quality Editorial service
- Swift Peer Review
- Reprints availability
- E-prints Service
- Manuscript Podcast for convenient understanding
- Global attainment for your research
- Manuscript accessibility in different formats  
( Pdf, E-pub, Full Text, Audio)
- Unceasing customer service

Track the below URL for one-step submission  
<https://juniperpublishers.com/online-submission.php>